Oxidative Dehydrogenation of Alkanes over V-based Catalysts: Influence of Redox Properties on Catalytic Performance

J. M. López Nieto,*,1 J. Soler,† P. Concepción,* J. Herguido,† M. Menéndez,† and J. Santamaría†

*Instituto de Tecnología Química, UPV-CSIC, Avda los Naranjos s/n, 4622 Valencia, Spain; and †Departamento de Ingeniería Química y T.M.A., Universidad de Zaragoza, 50.009 Zaragoza, Spain

The activity and selectivity of the catalysts used in oxidative dehydrogenation of alkanes results from a combination of factors related to the nature of the catalysts and to the operating conditions under which these are used. In this work, the oxidative dehydrogenation of alkanes (mainly butane) over V–Mg–O and VO$_x$/Al$_2$O$_3$ catalysts has been studied. The investigation is focused on the examination of the oxidation and reduction processes that take place on the surface of both catalysts. A combination of catalyst characterization and kinetic measurements has been used, in an attempt to relate the rate of these redox processes to the catalytic performance observed under oxidative dehydrogenation conditions. © 1999 Academic Press

Key Words: oxidative dehydrogenation of propane and *n*-butane; vanadium catalysts (alumina supported vanadia, vanadium-magnesium mixed oxides); redox properties.

INTRODUCTION

A number of catalytic systems have been reported recently as active and selective for the oxidative dehydrogenation (OXDH) of short chain alkanes, although only a few show a relatively high yield to the corresponding olefins (selectivities of at least 30–40% at alkane conversions of 50%) (1–6). V-based catalysts are firmly established among the most selective systems, although their selectivity to oxydehydrogenation products depends among other factors on the specific alkane fed, on the vanadium content of the catalysts, and on the nature of the matrix and/or support in which the vanadium atoms were incorporated (1). A review of the recent literature shows that the best performances in oxidative dehydrogenation of short chain alkanes have been obtained with V–Mg–O mixed oxides (4–12) and Al$_2$O$_3$-supported vanadia (13–17). However, while V–Mg–O mixed oxides catalysts seem to be the most active and selective catalysts in the OXDH of propane and *n*-butane, they show a low selectivity to ethene during the OXDH of ethane (6, 18, 19). In an opposite trend, Al$_2$O$_3$-supported vanadium oxide catalysts appear to be one of the most active catalysts in the OXDH of ethane (14, 15) and propane (13, 16) but their selectivity to C$_4$-olefins during the OXDH of *n*-butane is low (15, 20).

In both cases highly dispersed V^{5+} in a tetrahedral environment have been proposed as the selective sites, although the nature of active and selective sites and the influence of some characteristic of the catalysts used (acid-base, redox, promoters, etc.) is still under discussion. Thus, it has been recently proposed that the acid-base character of the catalysts could influence the selectivity-determining step which in turn is probably related to the adsorption/desorption of the olefinic intemediates and the reaction products (1).

On the other hand, it seems reasonable that the catalytic activity and stability are strongly influenced by the redox properties of the catalyst. These depend not only on the intrinsic characteristics of the solid, but also on the specific conditions under which the catalyst is used. The aim of this paper is to compare the redox properties of selective catalytic systems, i.e., V–Mg–O and VO$_x$/Al$_2$O$_3$ catalysts, and relate the results of the study to the observed behaviour during OXDH of *n*-butane. The catalytic results obtained in the OXDH of ethane and propane will be used as a reference in the discussion.

EXPERIMENTAL

Supported vanadium oxide catalysts (V–MgO or VO$_x$/Al$_2$O$_3$) were prepared by impregnation of the corresponding support with ammonium metavanadate aqueous solutions (12, 15). Commercial Al$_2$O$_3$ (Gidler T126; $S_{BET} = 188$ m^2 g^{-1}) and MgO ($S_{BET} = 140$ m^2 g^{-1}) prepared in our laboratory (12) were used as supports. The catalysts were dried at 80°C for 16 h and calcined at 600°C for 4 h. The characteristics of catalysts are shown in Table 1. Chemical analysis of Al, Mg, and V was carried out by atomic absorption spectroscopy.

Temperature-programmed reduction (TPR) results were obtained in a Micromeritics apparatus loaded with 20 mg of catalyst. The samples were first treated in argon at room

---

<div align="center">

TABLE 1

Characteristics of Vanadium-Based Catalysts

</div>

Catalyst	V-content (wt% V_2O_5)[a]	S_{BET} (m^2 g^{-1})	H_2-consumption (10^4 mol g^{-1})[b]	AOS[c]	Normalized oxygen consumption after reduction[d]		
					450°C	500°C	550°C
V–Mg–O	23.1	103	17.6	3.6	1.0	6.67	9.55
VO$_x$/Al$_2$O$_3$	7.14	137	6.65	3.1	1.0	1.02	1.06

[a] V-content of calcined catalysts.
[b] H_2-consumption during TPR experiments.
[c] Average oxidation state after the TPR experiments.
[d] Oxygen consumption at 450°C = 1.

temperature for 1 h. The samples were subsequently contacted with an H_2/Ar mixture (H_2/Ar molar ratio of 0.15 and a total flow of 50 ml min^{-1}) and heated, at a rate of 10°C min^{-1}, to a final temperature of 1000°C.

The catalytic experiments in the oxidehydrogenation of C_2–C_4 alkanes were carried out in a continuous quartz fixed bed reactor. The catalyst charge was 0.1–0.5 g mixed with 8 g of Norton silicon carbide. The premixed feed contained an alkane, oxygen and helium, in a molar ratio of 5/20/75 (*n*-butane) or 4/8/88 (propane and ethane). The catalytic tests were conducted at atmospheric pressure in the 400–550°C temperature interval. The analysis of reactants and products was carried out by gas chromatography, using a dual-column arrangement (Chromosorb PAW and molecular sieve 5A). Oxygenate products other than carbon oxides were not observed in this work. Blank runs showed that, under the experimental conditions used in this work, the contribution of reactions taking place in the void spaces of the reactor (homogeneous reactions) can be neglected.

The catalyst reduction tests were carried out at atmospheric pressure in a C.I. Electronics MK2 thermobalance. To this end, 150 mg of catalyst (particle size 100–250 μm) were previously oxidized at 550°C for 15 min, in a mixture of O_2/N_2 with a molar ratio of 17/83. After purging with N_2 for 10 min, the solid was contacted with a premixed H_2/N_2 stream (H_2 concentrations between 20 and 40%) at the reaction temperature. Weight readings were registered at 1-s intervals. The amount of oxygen consumed during a given reduction process could also be measured in catalyst reoxidation experiments. To this end, and after reduction, pulses of known volume containing a measured amount of O_2 in N_2 were sent over the sample, at the reoxidation temperature. Between pulses, the sample was kept under inert (99.999% He) atmosphere. An on-line quadrupole mass spectrometer (HIDEN HAL 2/201) was used to determine oxygen consumption by following the evolution of the signals corresponding to mass 32 (oxygen) and 28 (nitrogen, which was used as an internal reference). Catalyst reoxidation was considered complete when oxygen consumption

in the pulses sent over the catalyst could no longer be detected.

The reoxidation kinetics were investigated in a quartz reactor (i.d., 6 mm). Before the experiments, the samples were degassed for 5 min and then reduced for 30 min at 550°C, using a mixture with a H_2/N_2 molar ratio of 10 and a total flow of 50 cm^3 min^{-1}. The catalyst was then purged with He and a gas mixture containing O_2 and N_2 was then stepwise introduced in the reactor. The signals corresponding to mass 28 (N_2, as a reference) and 32 (O_2) were continuously monitored to calculate the instantaneous rate of oxygen consumption during catalyst reoxidation. The experimental systems used for both catalyst reduction and reoxidation kinetic experiments typically gathered several thousand points in any given experiment (which considerably increased the statistical reliability of the parameters obtained from data fitting).

Pulsed reactant tests were also used to characterize the behaviour of a progressively reduced catalyst. These were unsteady-state reaction experiments, in which pulses containing *n*-butane (typically 70 μmol) were sent over the catalyst, using a 12.5 cm^3 min^{-1} flow of purified He as carrier. The catalyst samples (500 mg) were previously subjected to reduction and then reoxidation at 550°C, using, respectively, H_2/N_2 and O_2/N_2 mass flow controlled gas mixtures. The analysis of reactants (conversion) and products (selectivity) was carried out by on-line mass spectrometry.

RESULTS AND DISCUSSION

The catalyst characterization results, previously reported, indicate that tetrahedral V^{5+} species are the main vanadium species. However, it is know that while isolated VO$_4$ tetrahedron in both amorphous and crystalline (Mg$_3$V$_2$O$_8$) phases are only present on the V–Mg–O catalyst (9, 12), both isolated and polymeric tetrahedral V^{5+} species are observed on alumina-supported vanadia catalyst (15, 17).
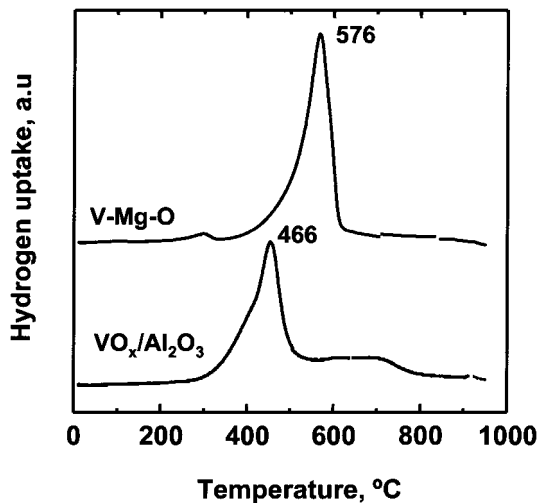
FIG. 1. Temperature-programmed reduction patterns of V–Mg–O and VO$_x$/Al$_2$O$_3$ catalysts. Conditions indicated in the text.

Catalyst Reducibility

Figure 1 presents the TPR patterns of V–Mg–O and VO$_x$/Al$_2$O$_3$ catalysts. It can be seen that the maximum for H$_2$ consumption in the alumina-supported catalyst appears at 110°C lower than in the V–Mg–O catalyst. This indicates that the reducibility of V-species in the V–Mg–O catalysts is lower than in the VO$_x$/Al$_2$O$_3$ catalyst.

Table 1 shows the H$_2$ consumption for both catalysts as well as the average oxidation state (AOS) obtained after the TPR experiments. It can be seen that V^{4+} species are formed after the reduction on the V–Mg–O catalyst. However, V^{3+} are formed after the reduction of the VO$_x$/Al$_2$O$_3$ catalyst. From these results, it can be concluded that V-species in VO$_x$/Al$_2$O$_3$ catalysts are more easily and more strongly reduced than those in a V–Mg–O catalyst.

In order to study the reduction rate of both catalysts, kinetic experiments were carried out at different temperatures and H$_2$/N$_2$ molar ratios. Figure 2 shows the progress of the reduction process for both V–Mg–O (Fig. 2a) and VO$_x$/Al$_2$O$_3$ (Fig. 2b) catalysts at hydrogen partial pressures of 0.2–0.4 and 550°C. Similar experiments (not shown) were performed at other temperatures. The kinetic parameters of reduction were calculated from the weight loss of 150 mg samples and transformed into the reduction degree (X_{red}) taking as $X_{red} = 0$ the initial state of the catalyst (which was previously oxidized at 550°C) and as $X_{red} = 1$ the state of the catalyst at the maximum weight loss observed. At 550°C, the total weight loss observed was 3.1 mg for V–Mg–O and 2.0 mg for the VO$_x$/Al$_2$O$_3$ catalyst, which corresponds to a final oxidation state of +4 or +3 for V–Mg–O and VO$_x$/Al$_2$O$_3$, respectively. Oxidation states of +4 (V–Mg–O) and +3 (VO$_x$/Al$_2$O$_3$) at $X_{red} = 1$ are in good agreement with the results of TPR experiments.

An increase in the partial pressure of hydrogen increases the reduction rate of both catalysts, although this is considerably faster for VO$_x$/Al$_2$O$_3$ at any of the compositions investigated (note the different x-axis scale in Figs. 2a and 2b). Thus, at the lowest hydrogen partial pressure used (0.2 atmospheres), reduction of the VO$_x$/Al$_2$O$_3$ catalyst is completed in about 13 min, while around 40 min were needed for V–Mg–O.

The effect of temperature on the reduction degree of V–Mg–O catalyst is presented in Fig. 3, where the curves corresponding to VO$_x$/Al$_2$O$_3$ at 300°C (only incipient reduction) and 550°C (the fastest reduction rate in this work) are also shown for comparison. The effect of temperature is remarkable: 50% reduction of V–Mg–O can be achieved in less than 5 min at 550°C, which increases to about 13 min at 500°C, and to nearly 50 min at 450°C. For both catalysts, the curves in Figs. 2 and 3 show a fast initial reduction rate, followed by a considerably slower reaction; the
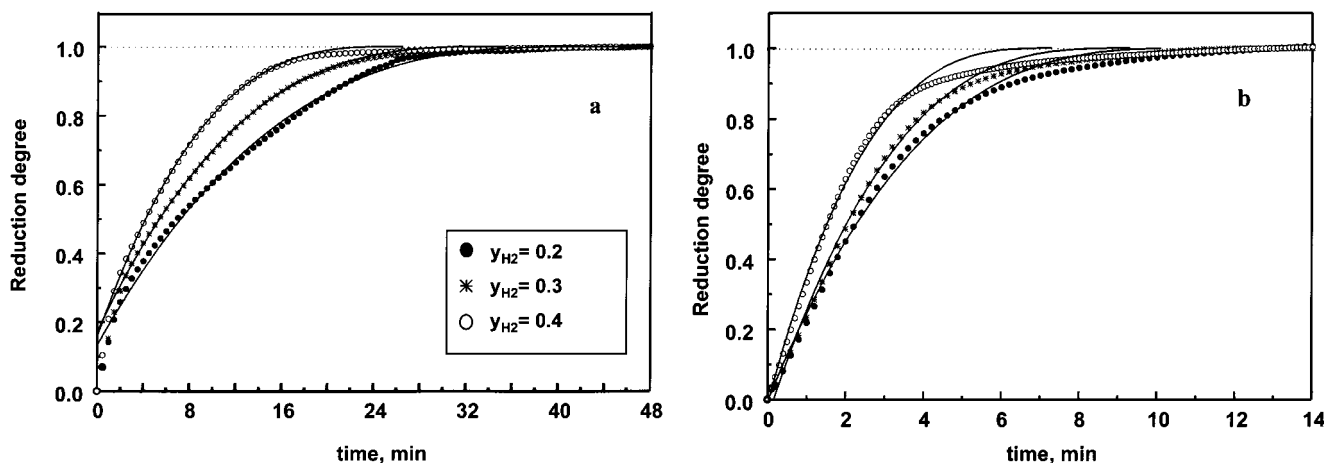

FIG. 2. Degree of catalyst reduction as a function of time on stream at 550°C for different hydrogen concentrations: (a) V–Mg–O; (b) VO$_x$/Al$_2$O$_3$. The continuous lines indicate the best fit by Eq. [1].
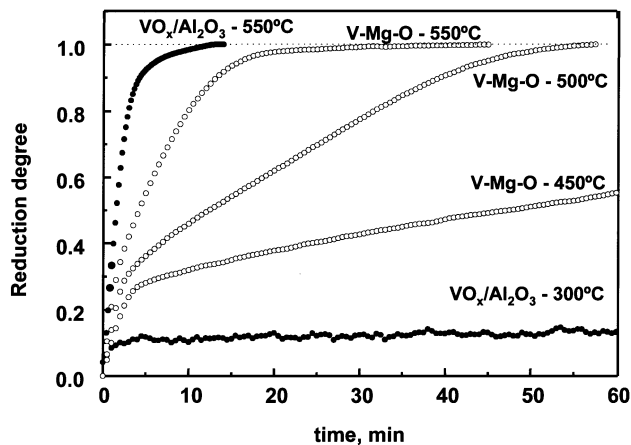
FIG. 3. Effect of temperature on the variation of the degree of catalyst reduction with time on stream; $P_{H2} = 0.40$ atm.

shape of the curves suggests that the reduction of the crystallites could be described according to the contracting core model. Equations corresponding to this model were in fact used previously by Sloczynski (22) to describe reduction and reoxidation of vanadia–titania catalysts. The contracting core model is consistent with a process in which a very fast nucleation occurs initially on the external surface of the crystallites, which results in a total reduction of the exposed V-atoms and the reduction process then progresses toward the crystallite center (21).

For both catalysts, the experimental data were fitted to

$$(1 - X_{red})^{1/3} = \alpha - (t/\beta) \qquad [1]$$

which is the same previously used by Sloczynski (22) to describe the reduction of TiO_2-supported vanadia catalysts with propane. When $\alpha = 1$ this equation is coincident with the contracting sphere model. The results of data fitting are given in Table 2, and fitting lines are shown along with

experimental data in Fig. 2. Table 2 shows that Eq. [1] gave a good fit of the experimental data for both catalysts. The calculated value of α was in all cases close to 1. β is inversely proportional to the intrinsic reaction rate. In addition, the β values given in Table 2 indicate that the reduction rate of VO_x/Al_2O_3 catalysts at 550°C is approximately 4 times faster than that of the V–Mg–O catalyst.

Some discrepancy between experimental and predicted values appears at high values of X_{red}, especially for the VO_x/Al_2O_3 catalyst (Fig. 2b). This corresponds to the reduction of the V atoms close to the centre of the crystallite, and the discrepancy can be explained as a consequence of increasing diffusion resistances through the external V-layers already reduced, which is not taken into account by Eq. [1]. The importance of this resistance would be greater for those catalysts where the intrinsic reduction rate is faster, which is consistent with the greater discrepancy observed for VO_x/Al_2O_3 catalysts in this case. For large grain sizes, it might be necessary to take into account this resistance which can be easily achieved by the introduction of a supplementary parameter, the effective diffusivity through the reduced layer, D_e. However, in our case Eq. [1] was able to predict reduction data up to conversions of at least 90% for both catalysts, and the introduction of an additional parameter was not deemed necessary.

On the other hand, the dependency of β with the partial pressure of hydrogen was very similar for both catalysts (Table 2), although β is also strongly dependent on temperature. Figure 4 shows the variation of β with temperature for different values of the hydrogen concentration during the reduction of V–Mg–O catalysts. An increase of temperature from 450 to 550°C reduces β roughly by a factor of 23 in the experiments carried out with 20% hydrogen concentration. The apparent activation energy calculated from the values in Fig. 4 was 145 kJ/mol, ($R = 0.997$), similar to that observed in other supported vanadia catalysts (22).
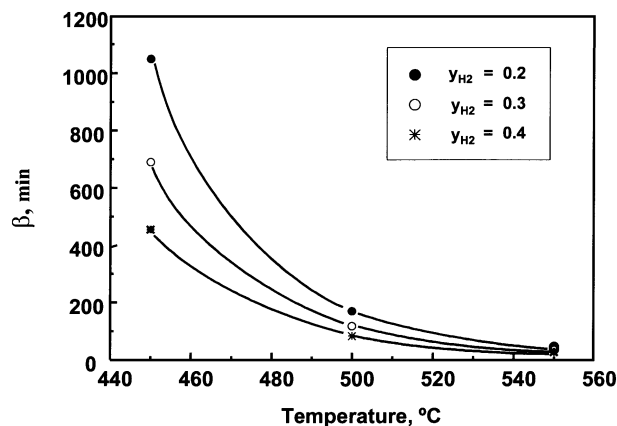
TABLE 2

Kinetic Constants for Reduction and Reoxidation of V–Mg–O and VO_x/Al_2O_3 Catalysts at 550°C

Catalyst	Reduction[a]				Reoxidation[b]			
	Y_{H2}	α	β	r	Y_{O2}	β	r	
V–Mg–O	0.2	0.954	45.2	0.998	0.050	2.010	0.997	
	0.3	0.940	37.0	0.998	0.075	1.127	0.996	
	0.4	0.946	27.5	0.998	0.100	0.714	0.999	
VO_x/Al_2O_3	0.2	1.002	10.9	0.998	0.500	0.291	0.998	
	0.3	1.018	9.0	0.999	0.750	0.236	0.999	
	0.4	1.005	7.2	0.998	0.100	0.178	0.996	

[a] according to Eq. [1] in text.
[b] according to Eq. [3] in text.

FIG. 4. Variation of β with reaction temperature and hydrogen concentration on the V–Mg–O catalyst.

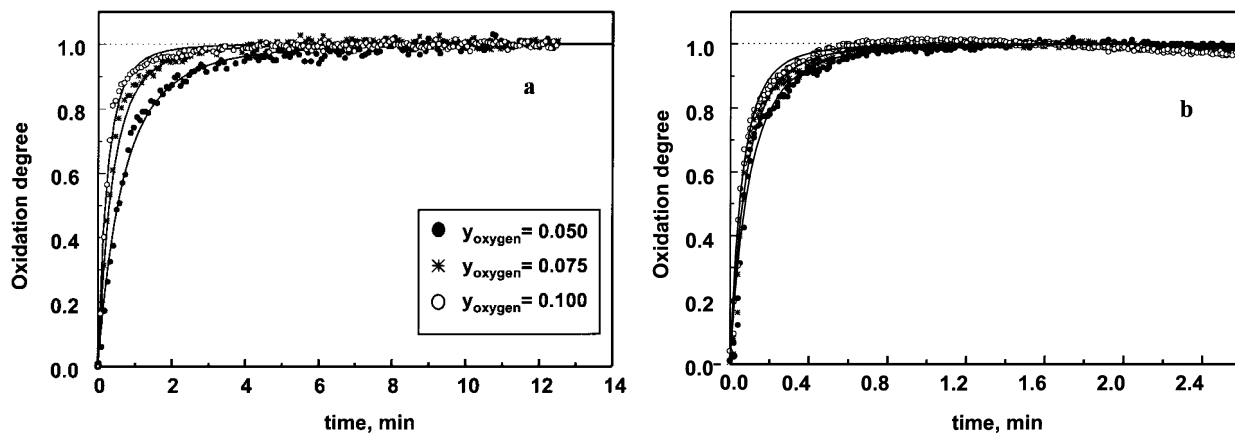**FIG. 5.** Degree of catalyst oxidation as a function of reaction time at 550°C for different oxygen concentrations: (a) V–Mg–O; (b) VO$_x$/Al$_2$O$_3$. The continuous lines indicate the best fit by Eq. 3.

Catalyst Reoxidation

Figure 5 shows the evolution of the degree of oxidation, X_{ox}, at 550°C for both V–Mg–O (Fig. 5a) and VO$_x$/Al$_2$O$_3$ (Fig. 5b) catalysts, respectively. In both cases, reoxidation experiments were carried out after reducing the catalyst at the same temperature used for reoxidation. As in the case of reduction, it can again be observed that the reoxidation of VO$_x$/Al$_2$O$_3$ catalysts takes place at a considerably higher rate than that of V–Mg–O. The kinetic data gathered during reoxidation were fitted to a kinetic equation similar to that proposed by Sloczynski for the VO$_x$/TiO$_2$ catalyst (22):

$$\left[(1 - X_{ox})^{-\frac{1}{3}} - 1\right]^2 = \alpha + \frac{t}{\beta} \quad [2]$$

Our data could not be fitted with this equation within the range of values with physical meaning (α should have null or positive values). However, a good fit was obtained by a modification of this expression, resulting in the following empirical equation:

$$(1 - X_{ox})^{-\frac{1}{3}} - 1 = \frac{t}{\beta} \quad [3]$$

The goodness of fit can be assessed from the statistics in Table 2 and the fitting lines in Fig. 5. It can easily be obtained that, in Eqs. 2 and 3, β represents the time necessary to obtain $X_{ox} = 0.875$. In this way, and from the comparison of the results obtained on both catalysts (Table 2) it can be concluded that reoxidation on the VO$_x$/Al$_2$O$_3$ catalyst is 4–7 faster than on the V–Mg–O catalyst. Also, for any of the two catalysts investigated, the reoxidation rate is 5–7 times faster than the corresponding reduction rate. Although some reports in the literature suggest that catalyst reoxidation is rate limiting (11), our results indicate that catalyst reduction rather than reoxidation could be rate limiting.

Table 1 compares the oxygen consumption during the reoxidation of catalysts that had previously been reduced at the same temperature used for reoxidation. In order to facilitate comparison, the amount consumed by each catalyst at the lowest temperature used (450°C) was taken as unity. Al$_2$O$_3$-supported vanadia catalyst showed an almost constant oxygen consumption throughout the temperature range investigated while, for V–Mg–O catalyst, the oxygen consumption increased strongly with the reoxidation temperature (increasing 10-fold when the temperature was raised from 450 to 550°C). These results could be explained as a consequence of either the low reduction rate or the low reoxidation rate observed for the V–Mg–O catalyst. However, we have shown above that the reoxidation of V on reduced V–Mg–O catalysts is considerably faster than its reduction. Since the TPR patterns indicate that the reduction of the V–Mg–O catalyst occurs significantly at temperatures of 500°C and above, a low catalyst reduction rate can be considered responsible for the formation of a low number of reduced V-species, which leads to a low oxygen consumption during reoxidation.

Figure 6 shows the variation of the *n*-butane conversion and the selectivity to C$_4$-olefins with reaction temperature during the OXDH of *n*-butane on V–Mg–O and VO$_x$/Al$_2$O$_3$ catalysts. In the experimental conditions used in Fig. 6 both catalysts show a similar *n*-butane conversion. However, it must be remembered that the V content of V–Mg–O catalysts is about 3 times that of VO$_x$/Al$_2$O$_3$, and the catalytic results were obtained at a contact time (W/F) on the V–Mg–O catalyst two times higher than on VO$_x$/Al$_2$O$_3$. Thus, it can be concluded that the intrinsic activity of V-atoms in VO$_x$/Al$_2$O$_3$ is higher than those in V–Mg–O. However, the advantage of the V–Mg–O catalyst is not on the activity but on the selectivity to OXDH products (C$_4$-olefins, including 1-, 2-*cis*-, and 2-*trans*-butene and
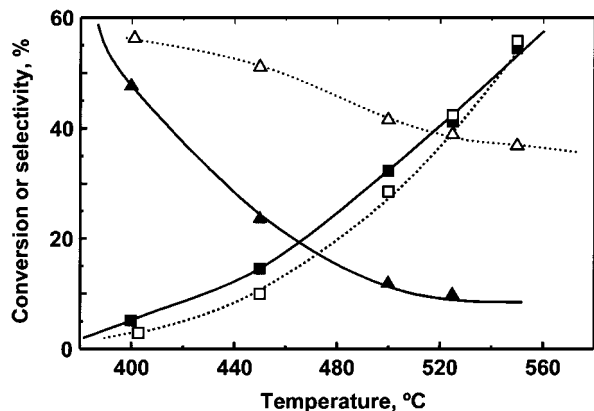
FIG. 6. Variation of the conversion of *n*-butane (■, □) and the selectivity to oxidehydrogenation products (▲, △) with the reaction temperature during the OXDH of *n*-butane on V–Mg–O (□, △) and VO$_x$/Al$_2$O$_3$ (■, ▲) catalysts. Experimental conditions: W/F = 10.7 (V–Mg–O) or 5.4 (VO$_x$/Al$_2$O$_3$) g$_{cat}$ h mol-C$_4^{-1}$.

FIG. 8. Variation of the selectivity to OXDH products with the *n*-butane conversions over V–Mg–O (◇, ○, □) and VO$_x$/Al$_2$O$_3$ (◆, ●, ■) catalysts at 500 (□, ■), 525 (▽, ▼), and 550°C (○, ●).

butadiene) which is more than 30 percentage points higher over that temperature interval.

Figure 7 shows the distribution of C$_4$-olefins, at approximately isoconversion conditions, obtained on both catalysts at 500 and 550°C. The formation of butadiene and 1-butene was favored on V–Mg–O, while the formation of 2-butene was favored on VO$_x$/Al$_2$O$_3$. In fact, a 1-butene/2-butene ratio between 1.1 and 1.3 was obtained for V–Mg–O in the experiments carried out in this work, while this ratio ranged between 0.5 and 0.6 on VO$_x$/Al$_2$O$_3$.

Figure 8 shows the variation of the selectivity to OXDH products with the conversion of *n*-butane for both catalysts, at three different temperatures. It can be seen that, in addition to the usual pattern of decreasing selectivity as the *n*-butane conversion is increased, which is typical in OXDH reactions, the selectivity to OXDH products also depends strongly on reaction temperature. Thus, at the same con-
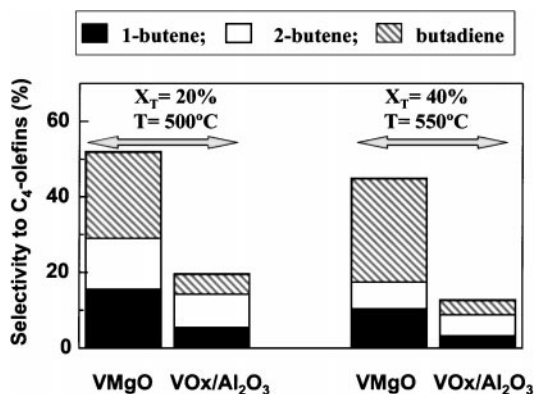
version, widely different selectivities can be obtained with the same catalyst, depending on the operating temperature. The beneficial effect of increasing the temperature seems to be more significant for V–Mg–O where, for instance, with an increase of temperature from 500 to 550°C the selectivity could be maintained stable while the conversion increased from less than 40 to over 60% (Fig. 8).

The results discussed in Figs. 6 to 8 correspond to experiments carried out under steady state conditions, with cofeeding of butane and oxygen to the reactor. It is also interesting to compare the behaviour of these catalysts under nonstationary anaerobic conditions, where the redox behaviour of the catalyst is more clearly displayed. This was carried out by sending a series of pulses of butane over a preoxidized catalyst and following the conversion of butane and the selectivity to the different products with pulse number. The butane conversion results at three different temperatures are displayed in Fig. 9. As could be expected, the conversion of *n*-butane is highest in the first pulse and then decreases for both catalysts as the amount of available lattice oxygen diminishes. However, a small but noticeable activity level was maintained even after 10 pulses of butane for V–Mg–O. Both results can probably be explained as the consequence of the higher V-content in V–Mg–O catalysts, which are then able to extend the supply of lattice oxygen for the reaction. The lattice oxygen reservoir on V–Mg–O catalysts makes their use possible in continuous redox reactors where the catalyst is continuously transferred from reduction zones (where lattice oxygen is consumed in the reaction) to oxidizing zones, where lattice oxygen is restored (23, 24).

Figure 10 shows the relative variation of the selectivity to CO$_2$ ($m/e = 44$) CO + C$_2$H$_4$ ($m/e = 28$), and butenes ($m/e = 56$). It can be seen that the selectivity to butenes increases with the number of pulses. This seems to indicate that a certain degree of catalyst reduction could be required

FIG. 7. Product distribution obtained during the OXDH products with *n*-butane conversions over V–Mg–O and VO$_x$/Al$_2$O$_3$ at 500 and 550°C and *n*-butane conversions of 20 and 40%, respectively.
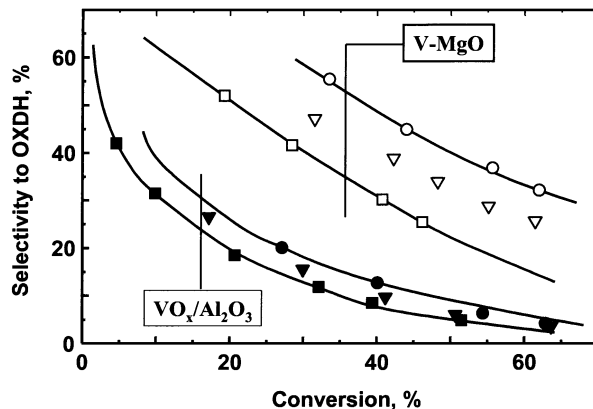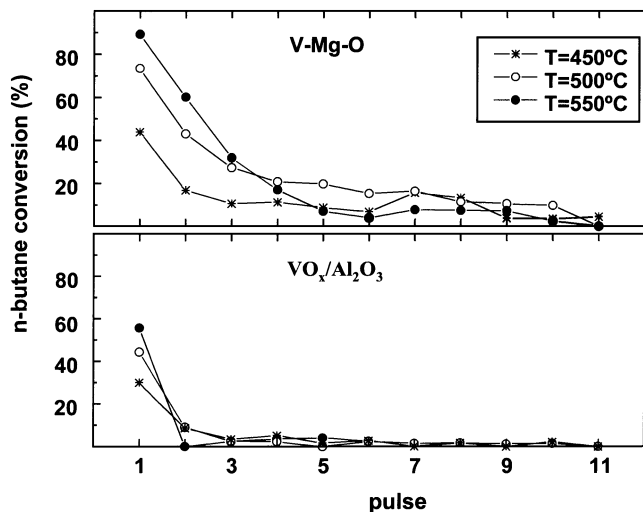
FIG. 9. Variation of butane conversion with pulse number for V–Mg–O and VO$_x$/Al$_2$O$_3$ at three different temperatures. Experimental conditions: Catalyst sample, 500 mg (particle size 100–250 μm); pulses, 70 μmol of n-butane; carrier flow-rate: 12.5 ml min^{-1} of He.

in order to obtain good selectivity. However, there is also the possibility that adsorbed oxygen (which has a mainly nonselective contribution) could remain on the V–Mg–O surface. In this case, a selective catalyst surface would be obtained only after the adsorbed oxygen had been consumed by the first butane pulses.

The experiments presented in this work do not allow confirming or rejecting the second hypothesis. However, some indirect support can be gathered from recently published oxygen isotopic-exchange experiments on a selective V–Mg–O catalyst, which showed that significant isotopic-exchange took place only at temperatures above 750 and 350°C on preoxidized and prereduced samples, respectively (12). This means that, at the temperatures used in this work, the incorporation of oxygen species on V–Mg–O catalyst
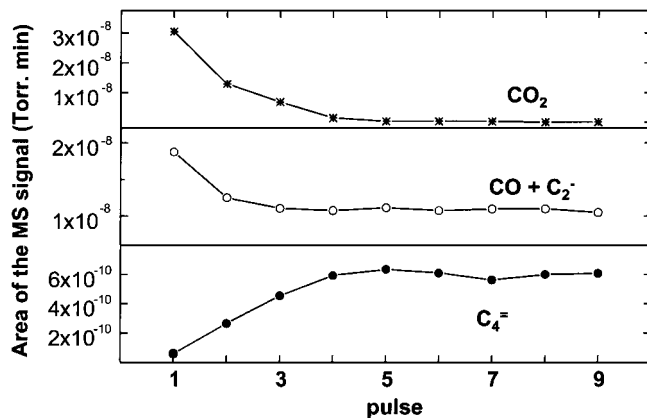

FIG. 10. Relative variation of the product distribution with pulse number for V–Mg–O at 550°C. Experimental conditions as Fig. 9.

should be carried out only on a reduced catalyst. However, the presence of adsorbed molecular oxygen species on the surface of an oxidized site cannot be ruled out.

According to the catalytic results presented above, the oxidation of n-butane on both alumina-supported vanadia and V–Mg–O catalysts can be represented by Scheme 1, in which the formation of butenes and butadiene, via the formation of an olefinic intermediate, would be achieved through a redox mechanism (6, 11, 12). This has been recently confirmed by using an *in situ* redox fluidized bed reactor for the OXDH of n-butane (23, 24).

It has been proposed that the catalyst reoxidation step could be rate limiting in the OXDH of propane on VMgO catalysts (11). However, and according to our results (the reoxidation can be 5–7 faster than reduction), only the catalyst reduction could be considered as the rate limiting step in the OXDH of n-butane. In fact, it is not casual that, on VMgO catalyst high selectivities to OXDH products can be only achieved at reaction temperatures higher than 500°C, a temperature near to that in which the catalyst reduction occurs with a relatively high reduction rate.

On the redox sites the mechanism would be initiated by hydrogen abstraction forming a butyl radical, as proposed by Kung *et al.* for V–Mg–O mixed oxides (6), which could then interact with the vanadium species, forming an adsorbed olefinic intermediate. The variation of the initial selectivity to C$_4$-olefins with the reaction temperature would be mainly related with the reducibility of the catalyst, which determine the rate of redox process and the k_1/k_1' ratio.

On the other hand, the formation of carbon oxides would take place via a different mechanism. Thus, Andersson (25) proposed that the deep oxidation of propane on VO$_x$/AlPO$_4$ could occur on V-free sites, involving the formation of a carbenium ion. The formation of deep oxidation products in our case could be explained by a similar alternative mechanism involving the presence of adsorbed oxygen (12, 26). Nevertheless, deep oxidation of olefins (k_2', k_3' and k_4' in Scheme 1) must also be considered at high butane conversions.

According to this, the selectivity observed under a certain set of reaction conditions would be given by the relative rates of selective (redox) to nonselective processes (k_1/k_1' ratio; competitive reactions) as well as by the nature of consecutive reactions. Operating conditions that facilitate the redox activity of the catalyst should then result in a higher selectivity to the desired products. In this way, it has been shown that a higher reaction temperature results in a higher selectivity to dehydrogenation products on both catalysts, although this effect is more important over the V–Mg–O catalyst (Fig. 8).

In previous works, it has been suggested that the beneficial influence of the reaction temperature on the selectivity to OXDH products could be a consequence of a higher activation energy for the selective oxidation reaction
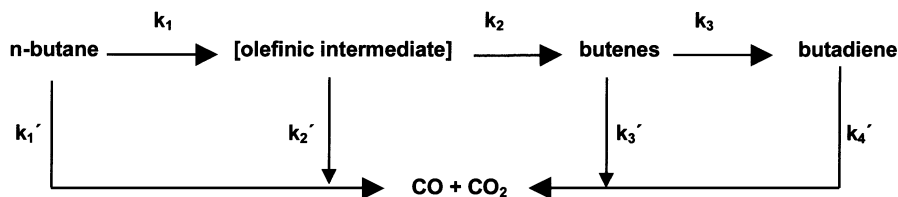
Scheme 1. Reaction network for the OXDH of *n*-butane.

(27, 28). From the results presented here, a more fundamental explanation seems possible: a low reducibility and a low catalytic activity of redox sites is expected at low reaction temperature. However, under reaction conditions, a higher temperature strongly increases the rates of the reduction process, and thus it would result in an enhancement of the redox capabilities of the catalyst.

It has been observed that the initial selectivity to olefins during the OXDH of short chain alkanes over V–MgO catalysts decreases when the number of carbon atoms of alkane decreases (18, 19) while an opposite trend has been observed in the case of VO_x/Al_2O_3 catalysts (15). In this case, the variation of the initial selectivity, and the ratio between selective (redox) and nonselective reactions on vanadium-based catalysts, could be partially explained on the basis of the alkane reactivity and the catalyst reducibility. Thus, it is clear that the OXDH of ethane (which presents a low reactivity) on V–Mg–O (which shows a low reducibility) is not favoured.

Figure 11 shows the selectivity to OXDH products obtained, under comparable conditions, during the oxidation of C_2–C_4 alkanes on both V–Mg–O and VO_x/Al_2O_3 catalysts. It can be seen that the selectivity to OXDH products in V–Mg–O decreases with the number of carbon atoms of the alkane fed, but it increases in VO_x/Al_2O_3.

Although the catalyst reducibility can determine the nature of competitive reactions (k_1/k_1' ratio), the selectivity to OXDH and the nature of consecutive reactions depend also on the nature of vanadium species (6–10, 19) and the acid-base character of catalysts (1, 18, 20). Nevertheless, these factors are also related to the alkane fed.

Michalakos *et al.* (19) proposed that the low selectivity to butenes during the oxydehydrogenation of *n*-butane on $Mg_2V_2O_7$-containing V–Mg–O catalysts is a consequence of the simultaneous attack of contiguous vanadium species (V–O–V) to terminal carbon atoms in butyl intermediates. This concept could be used in the OXDH of *n*-butane but not for the OXDH of ethane or propane.

CONCLUSIONS

The catalytic performance of OXDH catalysts is the result of a complex interaction involving a number of factors. In a previous work (1) it has been shown that the acid-base character of a catalyst in relation to the size of the alkane fed molecule plays a critical role in determining the selectivity to OXDH products. Also, the aggregation state of V-atoms on the surface could have a direct influence on the selectivity to C_4-olefins, since the length of V–O–V groups could match the length between terminal C-atoms of the alkane (6, 19).

This work attempts to bring an extra factor into consideration. We have observed that the reducibility of the V-atoms can influence the selectivity to OXDH products, and we have suggested that this could be explained by its effect on the rate of the selective redox processes involving V-species on the catalyst surface. Thus, in the case of *n*-butane, a higher reaction temperature accelerates redox exchanges on the catalyst, which results in a notably higher selectivity, especially on V–Mg–O whose reducibility is lower than that of VO_x/Al_2O_3. The same mechanism could be invoked in reverse form to explain the low selectivity to ethene from ethane observed on V–Mg–O. In this case, the relatively low reducibility of the catalyst is coupled with an alkane with low reactivity, resulting in a low activity in the transformation of ethane to ethene by a redox mechanism. This can be partially offset by an increase in the reaction temperature, which effectively increases the selectivity (27). Thus,

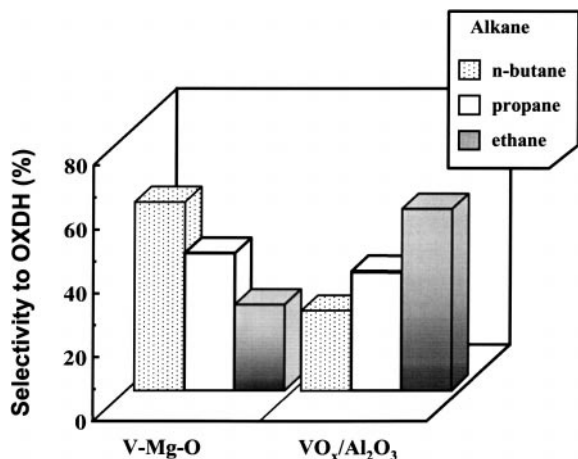**FIG. 11.** Selectivity to oxidehydrogenation products for V–Mg–O and VO_x/Al_2O_3 catalysts using different reactant molecules at 550°C and an alkane conversion of 30%. Experimental conditions: alkane/oxygen/helium molar ratio of 5/20/75 (*n*-butane) or 4/8/88 (propane and ethane).

the rate at which redox processes take place on the catalyst becomes another relevant factor in determining the catalytic performance of V-based oxidative dehydrogenation catalysts. Further work is needed to elucidate the strength of this effect and its relationship to other factors affecting catalytic performance.

ACKNOWLEDGMENT

REFERENCES

1. Blasco, T., and López Nieto, J. M., *Appl. Catal. A: General* **157**, 117 (1997).
2. Albonetti, S., Cavani, F., and Trifiro, F., *Catal. Rev. Sci. Eng.* **38**, 413 (1996).
3. Mamedov, E. A., and Cortés Corberán, V., *Appl. Catal. A: General* **127**, 1 (1995).
4. Cavani, F., and Trifiro, F., *Catal. Today* **24**, 307 (1995).
5. Moro-oka, Y., and Ueda, W., *in* "Catalysis, Vol.11: Specialist Periodical Reports," Chap. 6. Royal Society of Chemistry, Cambridge, UK, 1994.
6. Kung, H. H., *Adv. Catal.* **40**, 1 (1994).
7. Kung, H. H., and Chaar, M. A., US Patent 4772319, 1988.
8. Siew Hew Sam, D., Soenen, V., and Volta, J. C., *J. Catal.* **123**, 417 (1990).
9. Corma, A., López Nieto, J. M., and Paredes, N., *J. Catal.* **144**, 425 (1993).
10. Gao, X., Ruiz, P., Xin, Q., Guo, X., and Delmon, B., *J. Catal.* **148**, 56 (1994).
11. Pantazidis, A., Aurous, A., Hermann, J.-M., and Mirodatos, C., *Catal. Today* **32**, 81 (1996).
12. López Nieto, J. M., Dejoz, A., Vázquez, M. I., O'Leary, W., and Cunningham, J., *Catal. Today* **40**, 215 (1998).
13. Eon, J. G., Olier, R., and Volta, J. C., *J. Catal.* **145**, 318 (1994).
14. Le Bars, J., Auroux, A., Forisier, M., and Vedrine, J., *J. Catal.* **162**, 250 (1996).
15. Blasco, T., Galli, A., López Nieto, J. M., and Trifiró, F., *J. Catal.* **169**, 203 (1997).
16. Andersen, P. J., and Kung, H. H., *Stud. Surf. Sci. Catal.* **75**, 205 (1993).
17. López Nieto, J. M., Coenrads, R., Dejoz, A., and Vázquez, M. I., *Stud. Surf. Sci. Catal.* **110**, 443 (1997).
18. Concepción, P., Galli, A., López Nieto, J. M., Dejoz, A., and Vázquez, M. I., *Top. Catal.* **3**, 451 (1996).
19. Michalakos, P. M., Kung, M. C., Jahan, I., and Kung, H. H., *J. Catal.* **140**, 226 (1993).
20. Galli, A., López Nieto, J. M., Dejoz, A., and Vázquez, M. I., *Catal. Lett.* **34**, 51 (1995).
21. Hurst, N. W., Gentry, S. J., Jones, A., and McNicol, B. D., *Catal. Rev. Sci. Eng.* **24**, 233 (1982).
22. Sloczynski, J., *Appl. Catal. A: General* **146**, 401 (1996).
23. Soler, J., López Nieto, J. M., Herguido, J., Menéndez, M., and Santamaria, J., *Catal. Lett.* **50**, 25 (1998).
24. Soler, J., López Nieto, J. M., Herguido, J., Menéndez, M., and Santamaria, J., *Ind. Eng. Chem. Res.* **38**, 90 (1999).
25. Anderson, S. L. T., *Appl. Catal. A: General* **112**, 209 (1994).
26. Pantazidis, A., Bucholz, S. A., Zanthoff, H. W., Schuurman, Y., and Mirodatos, C., *Catal. Today* **40**, 207 (1998).
27. Dejoz, A., López Nieto, J. M., Melo, F., and Vázquez, M. I., *Ind. Eng. Chem. Res.* **36**, 2588 (1997).
28. Lemonidou, A. A., Tjatjopoulos, G. J., and Vasalos, I. A., *Catal. Today* **45**, 65 (1998).